

Heat Transfer Study of Liquid Nitrogen Jet Impinging on Granite Rocks

Ran Li, Xiaoguang Wu and Zhongwei Huang

State Key Laboratory of Petroleum Resources and Prospecting, China University of Petroleum (Beijing), Beijing 102249, PR. China

Keywords

Liquid nitrogen, Granite, Jet impingement, Boiling heat transfer

ABSTRACT

In this paper, we report an experimental study of liquid nitrogen (LN₂) jet impinging on granite rocks, aiming at figuring out the performance of LN₂ as a drilling fluid in the hot dry rock (HDR) formation. The focus is on the heat transfer aspects during jet impingement as the heat transfer directly dominates the resulted thermal stresses in rocks. The granite sample used is a square plate 24×24×2.5cm³ in size. It was cooled by LN₂ jet from room temperature at a jet pressure of 1.4-2.4MPa and a nozzle-to-surface distance of 3-5mm. The nozzle diameter was fixed at 1mm in present experiments. T-type thermocouples were inserted into the rock sample and the heat fluxes on rock surface were inversely solved using the measured temperature data.

It was found that during LN₂ jet the temperature distribution on the granite surface was not uniform. Instead, there was a wetted region around the stagnation point within which the temperature was dramatically lower than that in the outer region. The temperature gradient is the steepest at the front of this wetted region. With time elapsing, the granite is further cooled and the wetted region grows larger. By increasing the jet pressure or decreasing the nozzle-to-surface distance, the expansion of the wetted region becomes faster, thus accelerating the cooling rate of granite. The local heat flux rapidly increases with time at locations that are first reached by the front of wetted region. However, the peak values of heat flux become smaller for further locations. An empirical correlation was developed to predict the peak values of local heat flux which was strongly affected by radial distance and weakly influenced by nozzle-to-surface distance and jet pressure. The correlation can predict the peak values of heat flux within a relative error of ±10%.

1. Introduction

The success of the Enhanced Geothermal System (EGS) concept largely depends on the efficiency of rock breaking during either the drilling or fracturing processes. Drilling in hot dry rock (HDR) formation is extremely difficult due to the high temperature and high strength of granite rocks. For the same reason, it is also a great challenge to create artificial fracture networks in HDR formation for fluid circulation. Therefore, it is of significant importance to explore novel techniques to enhance the rock breaking capacity and efficiency in order to establish an economic EGS. This paper reports experimental results of liquid nitrogen (LN_2) jet impinging on granite rock surface focusing on the heat transfer aspects. In HDR drilling, the LN_2 can be used as the drilling fluid, impinging on the rock surface through the nozzles on the drilling bit. In fracturing, the LN_2 can take the place of water as in the water jet fracturing technique. The merit of using LN_2 is that the fracturing pressure threshold of reservoir rocks can be lowered (Cai et al., 2016).

In the oil and gas industry, researchers are exploring the possibility of using cryogenic liquids with ultra-low temperature to generate 'thermal shock' effects in rocks and to assist the generation of cracks (McDaniel et al., 1997, Grundmann et al., 1998, Yao et al., 2017, Cha et al., 2017, Wang et al., 2016). The best candidate for the working fluid is liquid nitrogen due to its inertial physical and chemical properties, natural abundance, low cost and being environmentally friendly. Laboratory experiments have been conducted to assess the change in petro-physical properties of rock samples after being frozen by LN_2 (Cai et al., 2014, Cai et al., 2015). Cha et al. studied the fracture initiation and propagation in sandstone blocks subject to LN_2 injection, either under free condition or under tri-axial confining pressure (Cha et al., 2014, Cha et al., 2018). The results of the abovementioned studies consistently demonstrate the positive role of the LN_2 -induced thermal stresses in creating cracks in rocks. In addition, Zhang et al. investigated the conjugate heat transfer between LN_2 jet and high temperature granites by the computational fluid dynamics (CFD) approach (Zhang et al., 2018a). They showed that the thermal stresses near the impact zone are in tensile state and the stress magnitude increases with jet velocity.

It should be expected that the LN_2 can generate more intense thermal shock effects and thus larger thermal stresses in HDR formation as the initial temperature of the HDR is higher than that of regular oil reservoirs. Further, it is apparent that the mechanisms and characteristics of the induced thermal stresses are related to the heat transfer from hot rocks to LN_2 flow. The evolution of heat transfer rates directly determines the temperature field in rocks and thus affects the distribution of thermal stresses. It is therefore necessary to study the transient heat transfer between rocks and flowing LN_2 , especially the LN_2 jet, to help understand the physical mechanism of rock breaking with LN_2 jet.

The only existing work in the literature addressing the heat transfer between LN_2 jet and rocks seems to be the two articles published by Zhang et al. (Zhang et al., 2018a, Zhang et al., 2018b) and the work was based on numerical simulation using commercial software. (Li et al., 2018) experimentally investigated the transient cooling of sandstone by LN_2 but the experiment was under static state, i.e., no movement of LN_2 . In this paper, we report experimental results on the heat transfer characteristics of LN_2 jet impinging on granite rock surface. Transient temperature field and surface heat flux profiles during the impingement are retrieved for the granite sample. Visualization data are also obtained to provide insights into the heat transfer process of LN_2 jet

impingement. The goal of present study is to shed light on the mechanism behind the thermal shock effects of LN₂ jet impinging on rocks.

2. Experiments and Data Reduction

2.1 Experimental Setup

Fig. 1 shows the schematic and photo of the present experimental setup which was designed to study the heat transfer characteristics of LN₂ jet impinging on rock surfaces under varied parameters. A self-pressurization LN₂ tank was used to produce the LN₂ jet. The tank is able to generate inner pressure up to 3MPa by vaporizing part of the LN₂ it stored. A pressure gauge was installed on the tank head to monitor the inner pressure which can be regulated through a needle valve (not shown in figure). The needle valve controls how much LN₂ is used for vaporization and thus how high the inner pressure will be. The LN₂ flow is directed to the nozzle through a flexible stainless-steel pipe. A bypass line is located just upstream the nozzle exit to allow temperature and pressure measurements of the LN₂ (see Fig. 1a). The inner diameter of nozzle was fixed at 1mm in this work and the nozzle-to-surface distance was varied between 3mm and 5mm. Two jet pressures of 1.4MPa and 2.4MPa were used to study the effect of jet velocity on heat transfer.

The granite sample is a square block with dimension of 24×24×2.5cm³ (see Figs. 2 & 4). Four holes 2mm in diameter were drilled in the sample to install the thermocouples (OMEGA, TT-T-24, 1mm in diameter). The locations of the holes are illustrated in Fig. 2 and the distance between hole bottom and the upper surface of granite was 5mm. In preliminary tests we have attempted to drill the holes to 2mm below the upper surface, but the measured temperature profiles showed abnormal trends. During impingement, the temperature at remote locations was even lower than that at the stagnation point, which is contrary to our instinct. It was possibly due to the nonhomogeneous property of granite rocks which contain numerous black mica embedded in feldspar and quartz. These minerals have different thermo-physical properties; if their size is close to 2mm then the temperature measurement will be affected by the non-homogeneity issue. The thermocouple adjacent to minerals with higher thermal conductivity will experience a faster temperature drop. This temperature drop, however, does not reflect the true heat transfer intensity. As a result, the hole was drilled to 5mm from the upper surface in subsequent experimental runs in order to eliminate the negative effect of non-homogeneity. The following results indicate that a thickness of 5mm was adequate for the granite layer to be considered as homogeneous and the average thermal properties can thus be used.

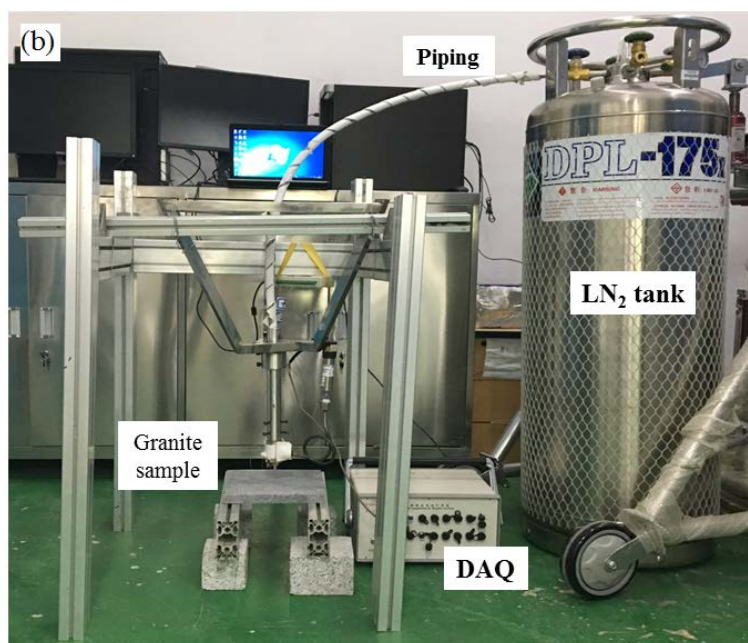
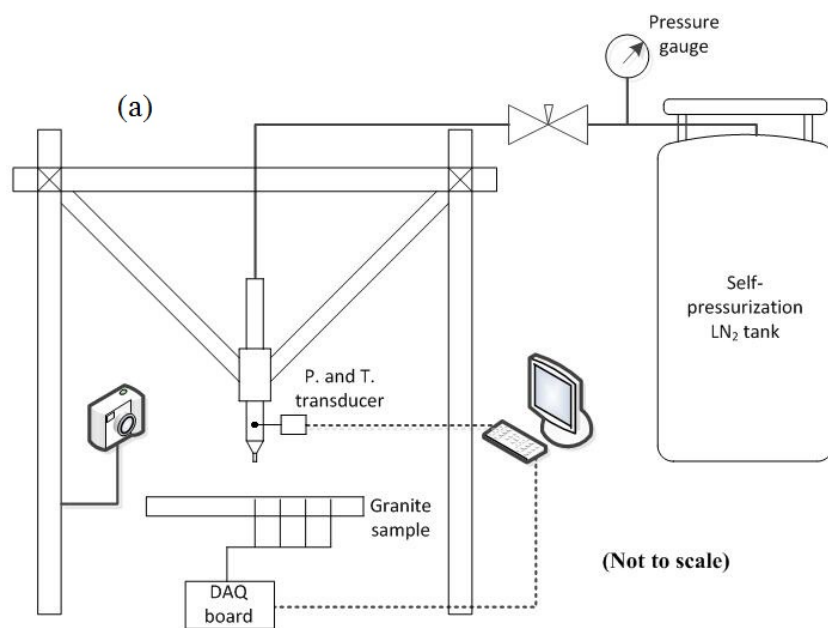


Figure 1: Schematic (a) and photograph (b) of the present experimental setup.

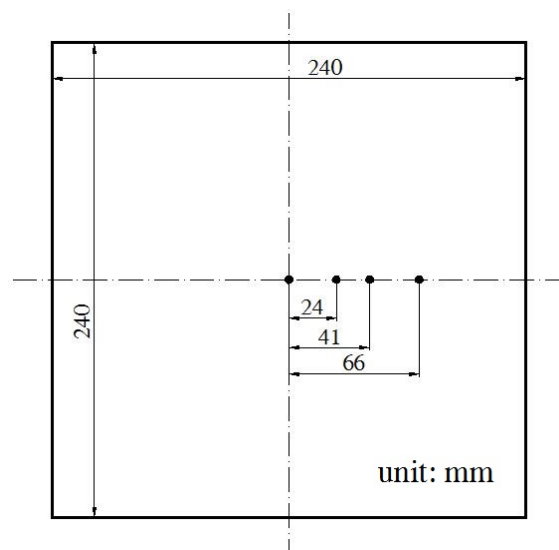


Figure 2: Schematic showing the dimension of the granite sample and locations of thermocouples. The thickness of granite is 2.5cm and the thermocouple tips are 5mm below the upper face of granite.

During experiments the pressure and temperature signals are processed by the data acquisition system (DAQ) and are recorded by the Labview program at 10Hz sampling rate. A digital camera was also employed to record the hydrodynamics of LN₂ jet impinging on granite surfaces at 60 frames per second. The digital images are synchronized with the temperature and pressure data and they can assist the analysis of experimental results.

The typical experimental procedure is as follows. First, the needle valve is adjusted to achieve the desired inner pressure in the LN₂ tank. The Labview program on the laptop is then initiated to start data acquisition. Before opening the exit valve to let out LN₂, a shutter covered with thermally insulating material was placed between the nozzle and the granite sample. Because a certain time period was needed to cool the piping system down to cryogenic temperature before ‘pure’ LN₂ jet comes out of the nozzle. The shutter can prevent the cool down of granite during this pre-cool stage. When the piping system is sufficiently cooled and the LN₂ jet is seen to be stable, the shutter is removed and the jet impingement is initiated. After the measured temperature under the stagnation point approaches the jet temperature, the experiment is terminated.

2.2 Data Reduction

The first-hand data obtained from the experiments are the measured temperatures by the four embedded thermocouples. From the viewpoint of heat transfer study, the transient heat flux distribution on the granite surface is of particular interest. Moreover, considering the thermal-shock effect produced by LN₂ jet, it is desired that the whole temperature field inside the granite sample be known. In theory, the abovementioned information cannot be precisely obtained unless sufficiently large number of temperature sensors are embedded in the granite and neglecting their influence on heat conduction. Obviously, this is impractical due to the limitation of experimental techniques. Alternatively, there is a compromise way to obtain the thermal information in the whole body of the sample using only four sensors; some assumptions are

required in this process, though. The method is based on inverse heat conduction technique and will be discussed only briefly here.

Taking the granite sample as the domain for a transient heat conduction system, its upper face is subject to an unknown heat flux which varies both with time and space. On the other hand, the boundary conditions on the bottom and four side faces can be evaluated using the heat transfer coefficient of free convection with air. To this end, the goal of the inverse heat transfer analysis is to find an appropriate heat flux profile $q(\mathbf{x}, t)$ for the upper face which can result in a temperature field agreeing best with the measured temperatures by thermocouples. The symbol $q(\mathbf{x}, t)$ means that the heat flux to be found is a function of both space and time.

In this work, the sequential least-square method developed by (Beck et al., 1985) was adopted to estimate the surface heat flux distribution during LN₂ jet impingement. The estimated surface heat flux is then used to reconstruct the temperature field in the granite. In short, the method of (Beck et al., 1985) temporarily assumed that the heat flux remained constant at some value for several time steps and that constant value is determined by minimizing the square error between calculated and measured temperatures. In this study, the axial symmetry of jet impingement was utilized to lower the dimension of problem. Before the temperature drop propagates to the periphery of the granite, we can approximate the temperature field as axisymmetric with respect to the stagnation point. Hence, the heat conduction is reduced to a two-dimensional problem under cylinder coordinate system.

The four thermocouples at discrete locations are inadequate to provide the complete information of the surface heat flux profile, as discussed by (Hall et al., 2001) and (Karwa et al., 2011). In fact, four sensors can only be used to estimate surface heat flux at four discrete locations. To map the spatial distribution of heat flux on the upper surface, some functional form for the heat flux distribution must be assumed. We assume that the heat flux varies linearly with space between two adjacent sensor locations. That is, a piecewise linear function has been used in the estimation of surface heat flux.

The uncertainties of the measured temperature and pressure in this work are $\pm 0.1^\circ\text{C}$ and $\pm 0.12\text{MPa}$, respectively. The thermo-physical properties of the used granite sample were also measured; the values and associated uncertainties are listed in Table 1. These properties are required in estimating the surface heat flux and in reconstructing the temperature field. Therefore, their uncertainties will propagate to the calculated heat flux results. Taking into account all the uncertainty sources, the final uncertainty of the estimated surface heat flux and temperature are determined to be within $\pm 15\%$ and $\pm 10^\circ\text{C}$, respectively.

Table 1: The thermo-physical properties of the granite sample.

	Thermal conductivity, W/m/K	Specific heat capacity, J/kg/K	Density, kg/m ³
Measured value	3.6	971.9	2630.23
Uncertainty	± 0.1	± 10	± 5

3. Results and Analysis

3.1 Cooling Curves

Fig. 3 represents the typical results obtained from one experimental run. The time-variation of temperature and pressure upstream the nozzle exit, and the transient cooling curves inside the granite are measured. The experimental condition was 1.4MPa for jet pressure and 5mm for nozzle-to-surface distance. As stated, the jet pressure is manually regulated via a needle valve therefore it is subject to certain fluctuations. Before $t=537s$ the shutter was in position and the temperatures in the granite remained at the initial level. This period is referred as pre-cooling stage during which the temperature upstream the nozzle (jet temperature) gradually decreases with time. In this stage, vapor and liquid alternatively flow out of the nozzle, accompanied by the instability of two-phase flow. As a result, the jet temperature shown in Fig. 3 shows an oscillation of high frequency between 100 and 450s. The amplification of the oscillation decreases with time and it ultimately vanishes which indicates that pure LN₂ jet is established and the first stage comes to an end. It is found that the duration of the pre-cooling stage is related to the jet pressure. At higher jet pressure the piping system cools faster and the pre-cooling stage is shorter. The ultimate jet temperature is found to be higher than $-195.8^{\circ}C$ (saturation temperature of LN₂ at atmospheric pressure) throughout all the experimental runs, which is likely due to the high pressure upstream the nozzle.

The impingement lasts for 230s for the test shown in Fig. 3. When the LN₂ jet impinges on the granite surface, the temperature under the stagnation point immediately drops at a high rate, which indicates a strong heat transfer at this point. For other positions far from the stagnation point, however, the temperature responses are somewhat delayed. A relatively gentle slope exists before drastic temperature drop. The further the location is from the stagnation point, the longer the delay is. For $r=66mm$, the temperature delay is the most evident. The temperature gradually decreases for $\sim 70s$ before the quick drop occurs. This trend of temperature variation is very similar to the static quenching curves reported by (Li et al., 2018). During the initial contact of LN₂ with rock, the heat transfer rate is low because of the existence of a vapor film which acts as a heat insulator. Later, the vapor film collapses resulting in a dramatic enhancement in heat transfer with direct liquid-solid contact. To better understand the temperature curves given in Fig. 3, the snapshots from the digital camera are used for analysis.

Fig. 4 presents a snapshot from the same experimental run as that shown in Fig. 3, i.e., under 1.4MPa jet pressure and 5mm nozzle-to-surface distance. The instant for the snapshot is 16s after impingement. In Fig. 4 the four thermocouple locations were marked by circular red dots; the thermocouple wires and the bypass line for pressure measurement are also shown in the snapshot. It is seen from Fig. 4 that the LN₂ jet expands after exiting the nozzle; the jet diameter is apparently larger than the nozzle diameter (1mm). This expansion is observed in all the experimental runs and should be related to the compressibility of nitrogen.

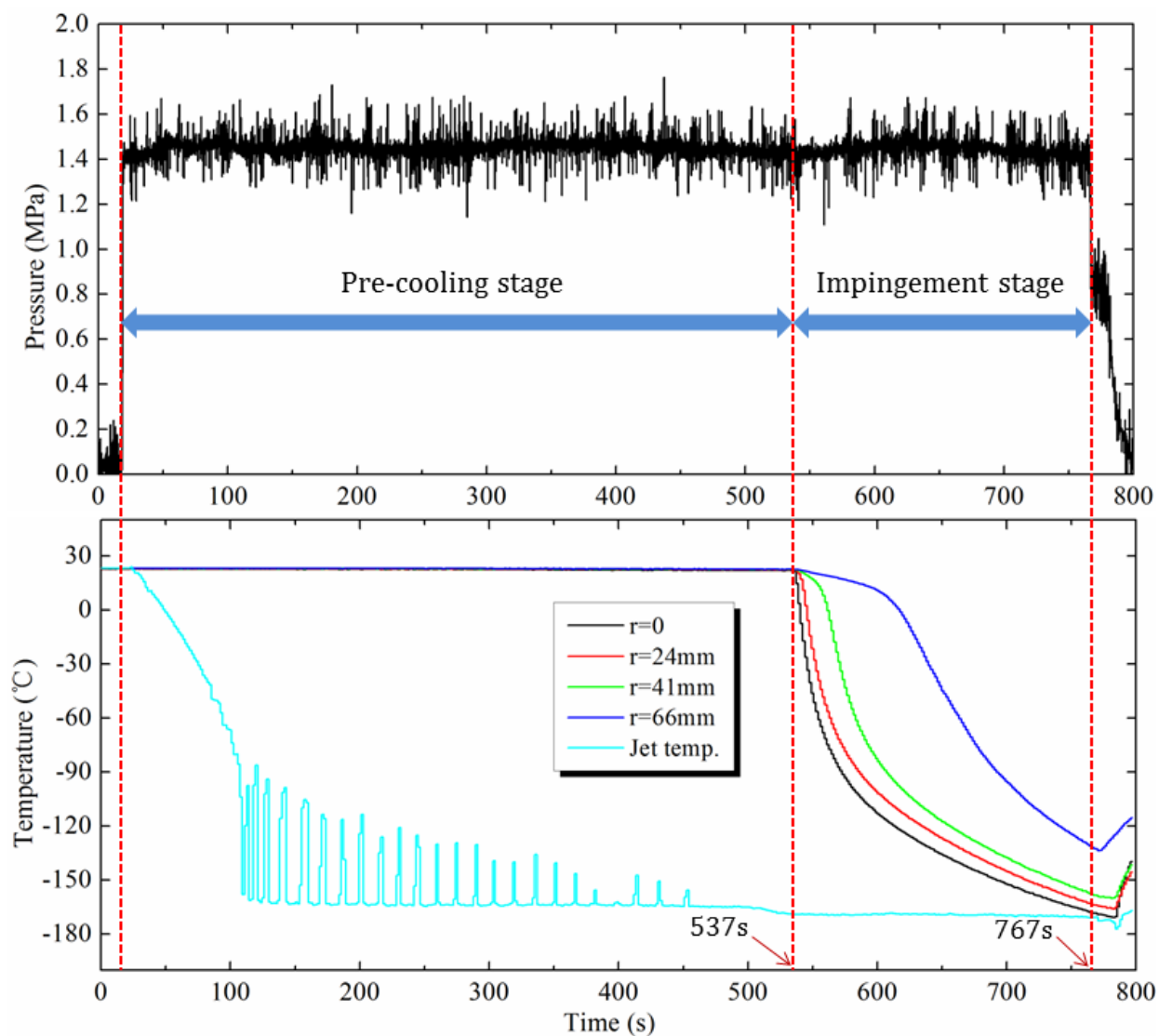


Figure 3: Pressure and temperature variation with time. One experimental run typically consists of two separate stages, i.e., the pre-cooling and the impingement stage. The jet pressure is ~1.4MPa and the nozzle-to-surface distance is 5mm for this figure.

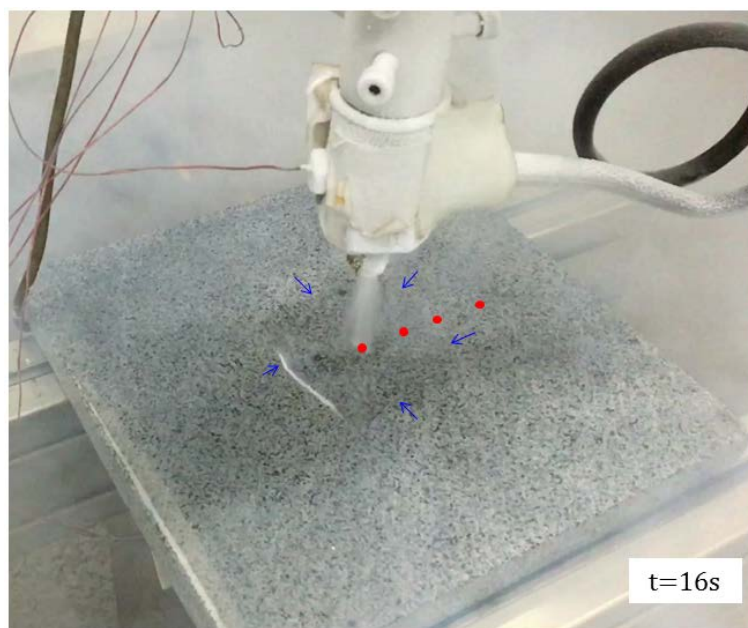


Figure 4: The snapshot showing the granite sample and the LN₂ jet. The circular red dots and blue arrows marked the positions of thermocouples and wetting front, respectively.

The most striking observation from the snapshot is the presence of a region around the stagnation point which was different in appearance from the outer regions. Within this region the *liquid* nitrogen is observed on the granite surface. Whereas outside this region only gaseous vapor was seen. The periphery of the region covered with liquid nitrogen is indicated by blue arrows in Fig. 4. Similar liquid-vapor interface evolution patterns can be found in studies of water jet impinging on hot metal surfaces (Hall et al., 2001, Karwa et al., 2011, Wang et al., 2016, Lee et al., 2017). Previous researchers referred to the region covered with water as ‘wetted region’ where the water is in contact with the solid surface and the heat transfer there is stronger than that in the dry region which is cooled by vapor and droplets. Therefore, in the present experiments we can describe the process of LN₂ jet impinging on granite in the same manner. As LN₂ jet strikes on the granite surface, the temperature around the stagnation point drastically decreases (see the $r=0$ curve in Fig. 3). The LN₂ can remain at liquid state within a small area around the stagnation point which can be called wetted region here. Outside this wetted region the temperature of rock is too high for the LN₂ to be liquid and it is replaced by nitrogen vapor. With time going on, the overall surface of granite is cooled off and the wetted region gradually expands.

Therefore, the time-delay of cooling curves shown in Fig. 3 can be attributed to the expansion of wetted region. Before a location is reached by the front of wetted region (wetting front), the surface is only cooled by cold vapor and the temperature thus drops gradually with time. When the wetting front arrives at that location the cryogenic liquid contacts the surface and greatly enhances the cooling rate. With the expansion of wetted region, the temperatures successively drop down at high rates along the radial direction. As seen in Fig. 4, the wetting front is about arriving at the third thermocouple location ($r=41\text{mm}$) and the temperature at this location sharply decreases shortly after this moment, as shown in Fig. 3. For the $r=66\text{mm}$ location, the wetting front spent a longer time to reach there because the moving velocity of wetting front decreases

with time. This is mainly due to the lower kinetic energy of LN₂ at locations further from the stagnation point. Therefore, the time delay of temperature response at the r=66mm location is the most striking in Fig. 3.

The expansion of the wetted region is influenced by the hydrodynamics of LN₂ jet. With more kinetic energy the LN₂ can overcome the retarding force and flow to a further location. The turbulence associated with high kinetic energy can also enhance the heat transfer, i.e., the cooling capacity of LN₂. As a result, the rock surface cools more rapidly and the wetted region grows faster if the kinetic energy of LN₂ jet is larger. Therefore, the stronger the hydrodynamics of LN₂ jet, the faster the wetted region should expand. Meanwhile, the wetted region expansion also influences the heat transfer; a faster expansion of wetted region will lead to a shorter delay in temperature response and hence an improvement of the overall cooling rate of the granite. From this argument, the expansion of wetted region and the heat transfer between LN₂ jet and rock influence each other in a conjugate manner.

Fig. 5 compares the cooling curves of granite sample under different nozzle-to-surface distances and jet pressures. To avoid crowding these results are presented in two separate figures and the curves in Fig. 3 were reused. It is clear from Fig. 5 that decreasing the nozzle-to-surface distance and increasing the jet pressure have the effect of accelerating the cooling of granite sample. The drastic temperature drop at further locations occurs earlier when increasing the jet pressure or decreasing the nozzle-to-surface distance because in these cases the hydrodynamics of LN₂ jet are stronger and the wetted region expands more quickly.

Fig. 5 also reveals that the effects of nozzle-to-surface distance and jet pressure are the most prominent at locations far from the stagnation point. For the r=0 and r=24mm locations, the cooling curves basically overlap. Under the present experimental conditions, the region of r<24mm can be called impact zone where the heat transfer is essentially unaffected by jet parameters.

3.2 Surface Heat Flux and Temperature Field

With the measured temperature profiles, the transient surface heat flux can be estimated using the inverse technique explained in section 2.2. The calculation results are presented in Fig. 6. Again, the curves are separated in two figures for clarity. The presented surface heat flux results are for the four thermocouple locations whereas the complete heat flux distribution on granite surface has to be attained using the piecewise linear function assumption.

It is seen from Fig. 6 that all the heat flux curves exhibit a similar time-variation trend but are successively delayed in time. The heat flux rapidly rises to a peak and then slowly drops down with time. Taking the observed movement of wetting front into account, it can be deduced that the rapid increase of heat flux at different locations signifies the arrival of LN₂ wetting front at that particular location. Another important finding from Fig. 6 is that the peak values of heat flux decrease dramatically with the increase of radial distance from stagnation point. The maximum heat flux ranges from 230 kW/m² at the stagnation point to approximately 60 kW/m² at the r=66mm location. As the LN₂ flows outward, its kinetic energy and velocity become smaller, thus reducing its capability to take away heat in unit time. The maximum heat flux in static cooling of sandstone by LN₂ was ~70 kW/m² (Li et al., 2018). Therefore the high velocity jet of LN₂ can enhance the heat transfer in the region of r≤41mm comparing to static cooling.

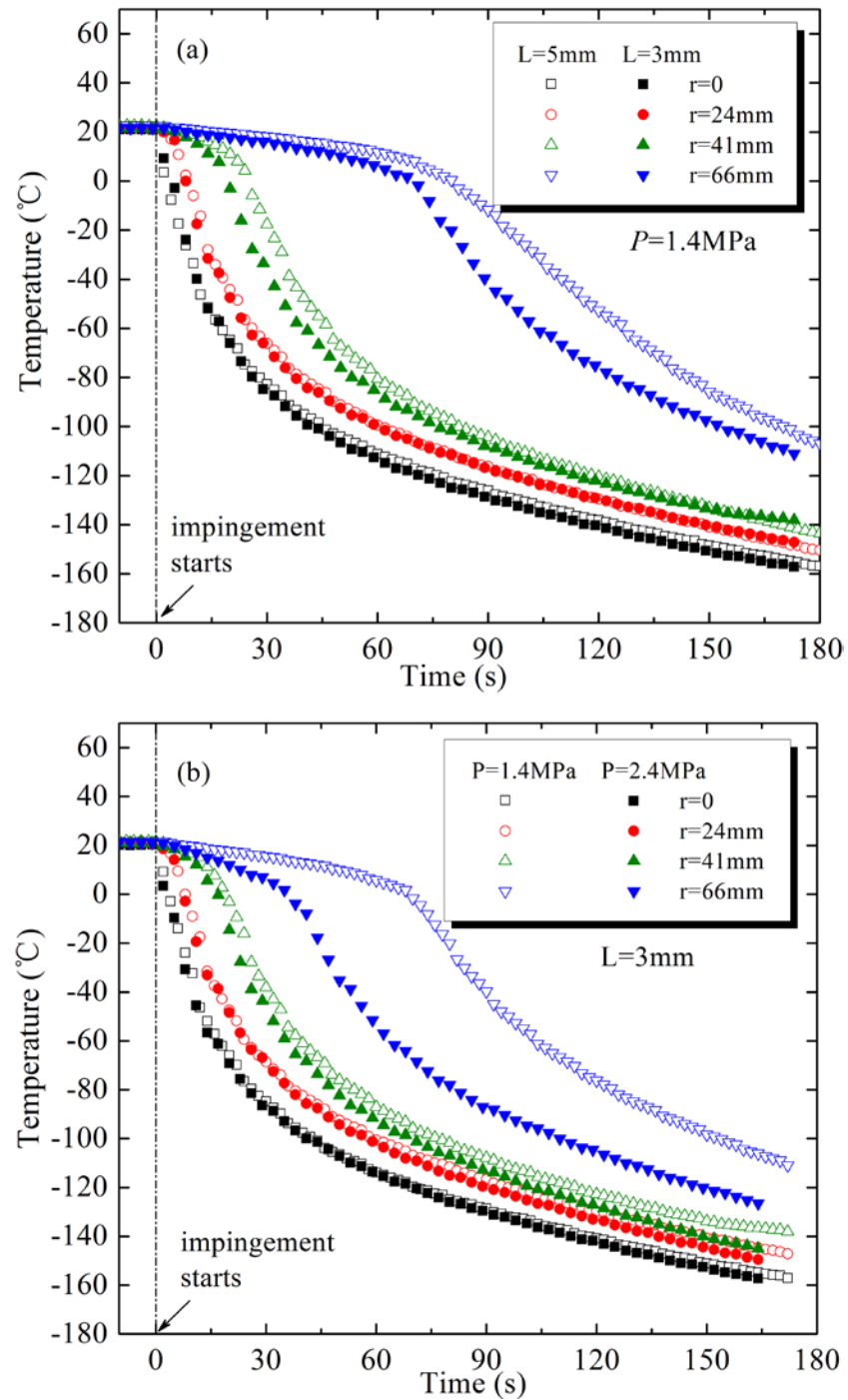


Figure 5: The effect of nozzle-to-surface distance (a) and jet pressure (b) on the cooling of granite by LN_2 jet. The jet pressure for (a) was 1.4MPa while the nozzle-to-surface distance was 3mm for (b).

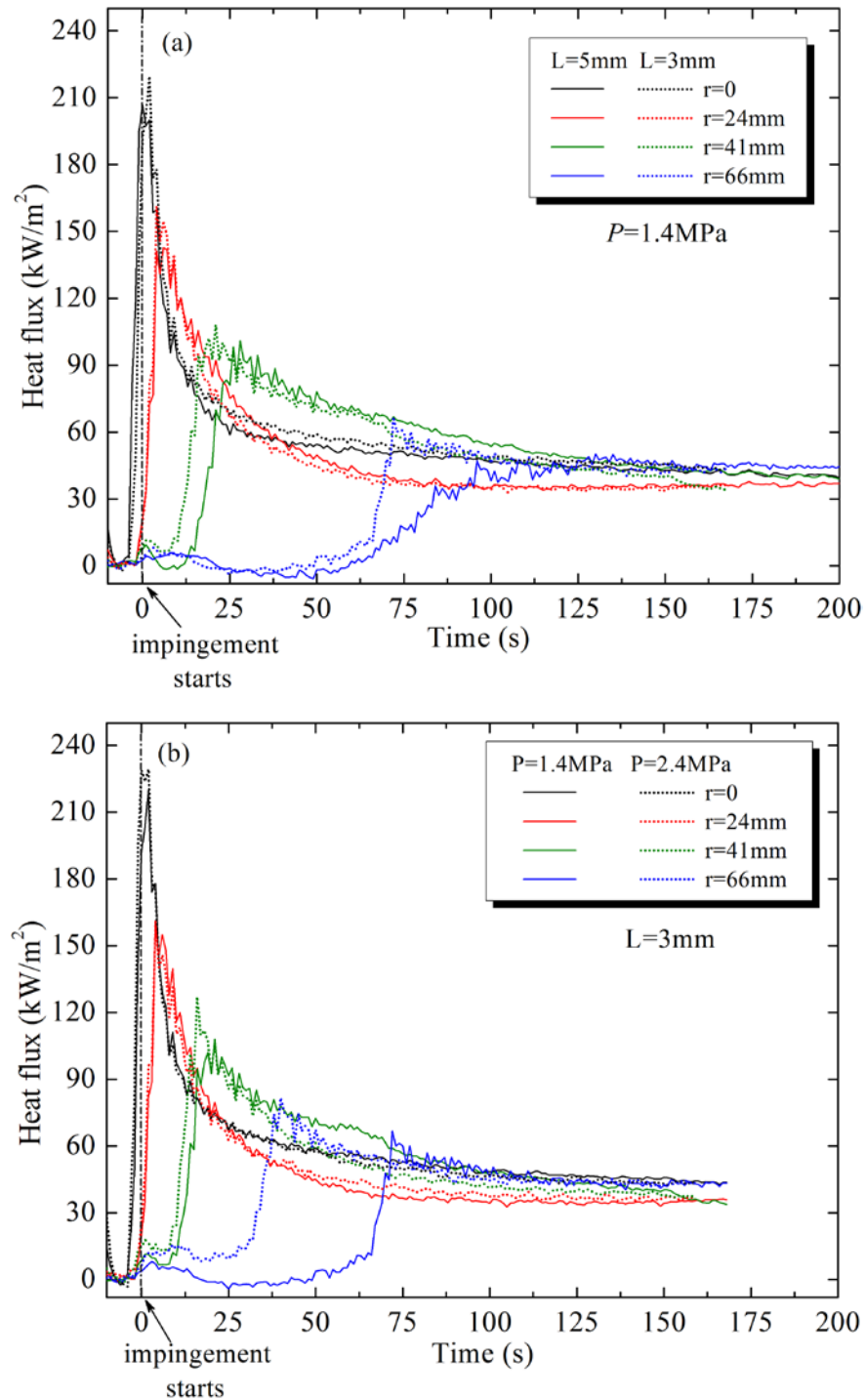


Figure 6: The effect of nozzle-to-surface distance (a) and jet pressure (b) on the surface heat flux. The jet pressure for (a) was 1.4MPa while the nozzle-to-surface distance was 3mm for (b).

The heat flux curves in Fig. 6 corroborate that the jet parameters basically have no influence on the heat transfer within 24mm radial distance, probably because the Reynolds number of LN₂ jet is relatively large in this work so that a further increase in jet pressure or decrease in nozzle-to-surface distance will not significantly change the heat transfer rate near the stagnation point. The Re was typically in the order of 10^4 in studies of water jet impinging on hot metallic surfaces. While in present study the Re is up to 4×10^5 (see section 3.3), an order of magnitude higher than that in water jet studies.

For further locations such as $r=41$ & 66 mm, the reduction of nozzle-to-surface distance and increase of jet pressure can both make the heat flux rise earlier. This is in line with the cooling curves given in Fig. 5. The reason is that the wetting front moves faster under smaller nozzle-to-surface distance and higher jet pressure.

The information about temperature field inside the granite block is valuable because the thermal stress is closely related to the inner temperature distribution. Fig. 7 shows the calculated temperature fields in the granite at two different moments, viz. 20s and 60s after impingement. The corresponding jet parameters are 1.4MPa for jet pressure and 5mm for nozzle-to-surface distance. Figs. 7a & 7b present the temperature distribution on the upper face of the granite while Figs. 7c & 7d show the temperature variation along the depth direction. It is seen that the zone with low temperature gradually expands with time, both in the horizontal and depth direction. In Fig. 7b the blue circle at the center represents the wetted region where the temperature is dramatically low ($< -130^\circ\text{C}$). Outside this wetted region there is an annular transition region. Further outside the transition region the temperature is close to the initial temperature. Therefore, the deepest temperature gradient is located in the transition region. Inside the wetted region and outside the transition region the temperature barely varies with position. While in the transition region the temperature sharply increases from a cryogenic level to approximately the initial level (room temperature). Referring to Fig. 5a, at $t=60$ s the temperature at 41mm location has dropped to a low level whereas the temperature at 66mm location is still high. Therefore, the wetting front at $t=60$ s should be between 41 and 66mm from stagnation point. This reasoning agrees well with the temperature contour shown in Fig. 7b. The transition region lies exactly between the 41 and 66mm locations.

The thermal stress is caused by the mismatch of thermal expansion inside a solid. A steeper temperature gradient results in more severe mismatch of thermal expansion and thus larger thermal stresses. Hence, the maximum thermal stress in the granite sample should be accord with the location of the transition zone and gradually moves away from the stagnation point with time. This conclusion is preliminary and needs validation through finite element analysis which will be done in the future work.

3.3 Correlation for Peak Values of Heat Flux

Fig. 6 has shown that the peak values of local heat flux decrease with radial distance. The peak value of local heat flux determines the magnitude of thermal stress induced at the same location. A higher peak heat flux corresponds to a steeper thermal gradient and larger thermal stresses. It is therefore useful to develop an empirical correlation to predict the peak values of local heat flux so as to provide knowledge about the thermal stress distribution.

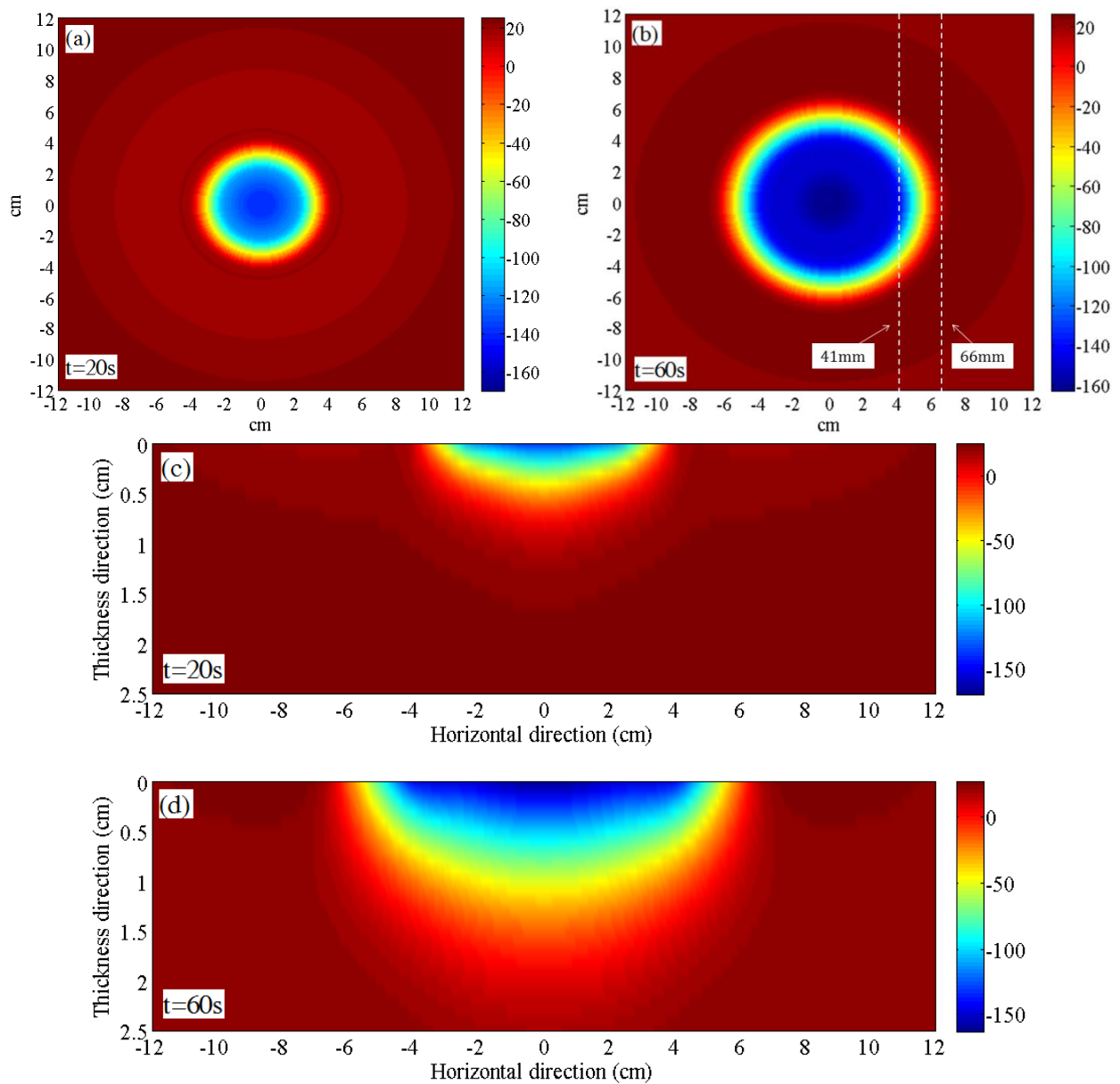


Figure 7: Temperature distribution in the granite sample at 20s (a & c) and 60s (b & d) after impingement. (a) and (b) show the temperature on the upper face while (c) and (d) show the temperature distribution along the depth direction. The results are for jet pressure of 1.4MPa and nozzle-to-surface distance of 5mm.

From Fig. 6, the peak value of heat flux is mainly influenced by radial distance; it decreases with the radial distance from the stagnation point. The reduction of nozzle-to-surface distance and increase of jet pressure can, on the other hand, marginally improve the peak heat fluxes. As a result, the peak heat flux is correlated with three independent parameters: the Reynolds number

of LN₂ jet, the dimensionless radial distance and the dimensionless nozzle-to-surface distance. The definitions of these parameters are

$$Re = \frac{u \cdot D}{\nu}, u = \sqrt{\frac{2P}{\rho_L}}$$

$$\text{dimensionless radial distance: } \bar{r} = \frac{r}{D} \quad (1)$$

$$\text{dimensionless nozzle-to-surface distance: } \bar{L} = \frac{L}{D}$$

where D is the nozzle diameter (1mm) and L is the nozzle-to-surface distance. It is noted that the calculation of Re by Eq. (1) neglects the expansion of LN₂ jet after exiting the nozzle. The nonlinear fitting tool in MATLAB was used to generate the following correlation for peak heat flux

$$q_{max} = 20441 \cdot Re^{0.205} \cdot e^{-0.017\bar{r}} \cdot \bar{L}^{-0.173} \quad (2)$$

where the q_{max} has the unit of W/m². The proposed correlation given by Eq. (2) is valid for LN₂ jet impinging on granite rock with jet pressure between 1.4MPa and 2.4MPa (Re between 294701 and 385854), nozzle-to-surface distance between 3 and 5mm and nozzle diameter of 1mm.

In the literature, the peak heat flux was normally correlated with the Re number along with the radial and nozzle-to-surface distances, in the following form (Sharma et al., 2018, Agrawal et al., 2012)

$$q_{max} = a_1 \cdot Re^{a_2} \cdot \bar{r}^{-a_3} \cdot \bar{L}^{a_4} \quad (3)$$

However, Eq. (3) is unable to account for the stagnation point because \bar{r} equals zero at the stagnation point. The exponent form adopted by the present correlation has no such difficulty. Fig. 8 plots the predicted peak values of heat flux using Eq. (2) against the experimental data. It shows that the proposed correlation can predict the peak heat flux very well with only one data point falling out of the $\pm 10\%$ confidence interval.

4. Conclusions

Heat transfer experiment of LN₂ jet impinging on granite rock surface was reported in this paper. The ranges of parameters are 1.4-2.4MPa for jet pressure and 3-5mm for nozzle-to-surface distance, respectively. The nozzle diameter was fixed at 1mm. An inverse heat transfer technique was employed to reconstruct the temperature field in and surface heat flux on the granite sample, which was cooled by LN₂ jet from room temperature. Generally, the results demonstrated the strong cooling capacity of LN₂ jet impinging on granite rocks. By creating a circular zone with low temperature around the stagnation point, the LN₂ jet assists the formation of thermal gradients and thermal stresses within the rocks. Thus, the LN₂ jet has potential in the drilling/stimulating work in the EGS field.

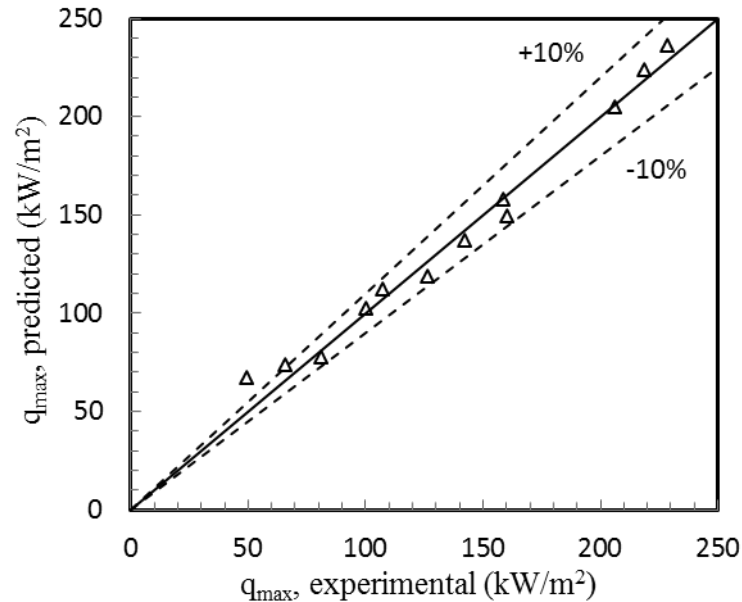


Figure 8: Comparison of predicted and experimental values of peak heat flux using the correlation proposed in present study.

A wetted region was observed around the stagnation point immediately after the impingement. The wetted region then continued to expand at a decreasing velocity with time. With the decrease of nozzle-to-surface distance and the increase of jet pressure, the wetted region expanded more rapidly, thereby reducing the delay of temperature response for locations far from the stagnation point.

At the front of the wetted region, the surface heat flux sharply rises with time and reaches to a peak value, which also leads to the steepest local temperature gradient and largest thermal stress. The maximum local heat flux was found to be 230 kW/m^2 , which was three times of the heat flux in static cooling of rock by LN_2 . The peak value of heat flux was found to decrease with radial distance and nozzle-to-surface distance and increase with the jet pressure. An empirical correlation was proposed which was able to predict the peak heat flux within 10% error.

It is noted that the present experiments were conducted under ambient conditions, i.e., room temperature and atmospheric pressure. If the heat transfer coefficient was not affected by temperature, then we can expect a stronger heat transfer between LN_2 jet and high temperature granite rocks because the temperature difference is wider in this case. Therefore, LN_2 jet can generate larger thermal stresses in granite rock with higher initial temperatures when the other mechanical boundary conditions are the same.

Acknowledgements

This work was supported by the National Natural Science Foundation of China (U1562212), the National Science Fund for Distinguished Young Scholars (No. 51725404) and the ‘111’ project of China (No. 110000203920170063).

REFERENCES

- C. Cai, Z. Huang, G. Li, F. Gao, J. Wei and R. Li. "Feasibility of reservoir fracturing stimulation with liquid nitrogen jet" *Journal of Petroleum Science and Engineering*, 144, (2016), 59-65
- B. W. McDaniel, S. R. Grundmann, W. D. Kendrick, D. R. Wilson and S. W. Jordan. "Field Applications of Cryogenic Nitrogen as a Hydraulic Fracturing Fluid" (1997)
- S. Grundmann, G. Rodvelt, G. Dials and R. Allen. "Cryogenic Nitrogen as a Hydraulic Fracturing Fluid in the Devonian Shale" *SPE Eastern Regional Meeting*, (1998)
- B. Yao, L. Wang, X. Yin and Y.-S. Wu. "Numerical modeling of cryogenic fracturing process on laboratory-scale Niobrara shale samples" *Journal of Natural Gas Science and Engineering*, 48, (2017), 169-177
- M. Cha, N. B. Alqahtani, X. Yin, T. J. Kneafsey, B. Yao and Y.-S. Wu. "Laboratory system for studying cryogenic thermal rock fracturing for well stimulation" *Journal of Petroleum Science and Engineering*, 156, (2017), 780-789
- L. Wang, B. Yao, M. Cha, N. B. Alqahtani, T. W. Patterson, T. J. Kneafsey, J. L. Miskimins, X. Yin and Y.-S. Wu. "Waterless fracturing technologies for unconventional reservoirs-opportunities for liquid nitrogen" *Journal of Natural Gas Science and Engineering*, 35, (2016), 160-174
- C. Cai, G. Li, Z. Huang, Z. Shen, S. Tian and J. Wei. "Experimental study of the effect of liquid nitrogen cooling on rock pore structure" *Journal of Natural Gas Science and Engineering*, 21, (2014), 507-517
- C. Cai, G. Li, Z. Huang, S. Tian, Z. Shen and X. Fu. "Experiment of coal damage due to supercooling with liquid nitrogen" *Journal of Natural Gas Science and Engineering*, 22, (2015), 42-48
- M. Cha, X. Yin, T. Kneafsey, B. Johanson, N. Alqahtani, J. Miskimins, T. Patterson and Y.-S. Wu. "Cryogenic fracturing for reservoir stimulation – Laboratory studies" *Journal of Petroleum Science and Engineering*, 124, (2014), 436-450
- M. Cha, N. B. Alqahtani, B. Yao, X. Yin, T. J. Kneafsey, L. Wang, Y.-S. Wu and J. L. Miskimins. "Cryogenic Fracturing of Wellbores Under True Triaxial-Confining Stresses: Experimental Investigation" *SPE Journal*, 180071-PA, (2018), 1-19
- S. Zhang, Z. Huang, G. Li, X. Wu, C. Peng and W. Zhang. "Numerical analysis of transient conjugate heat transfer and thermal stress distribution in geothermal drilling with high-pressure liquid nitrogen jet" *Applied Thermal Engineering*, 129, (2018a), 1348-1357
- S. Zhang, Z. Huang, P. Huang, X. Wu, C. Xiong and C. Zhang. "Numerical and experimental analysis of hot dry rock fracturing stimulation with high-pressure abrasive liquid nitrogen jet" *Journal of Petroleum Science and Engineering*, 163, (2018b), 156-165
- R. Li, Z. Huang, X. Wu, P. Yan and X. Dai. "Cryogenic quenching of rock using liquid nitrogen as a coolant: Investigation of surface effects" *International Journal of Heat and Mass Transfer*, 119, (2018), 446-459
- J. V. Beck, B. Blackwell and C. R. St. Clair. "Inverse Heat Conduction, Ill-Posed Problems" Wiley, (1985), 268-277

- D. E. Hall, F. P. Incropera and R. Viskanta. "Jet Impingement Boiling From a Circular Free-Surface Jet During Quenching: Part 1—Single-Phase Jet" *Journal of Heat Transfer*, 123, (2001), 901-910
- N. Karwa, T. Gambaryan-Roisman, P. Stephan and C. Tropea. "Experimental investigation of circular free-surface jet impingement quenching: Transient hydrodynamics and heat transfer" *Experimental Thermal and Fluid Science*, 35, (2011), 1435-1443
- B. Wang, D. Lin, Q. Xie, Z. Wang and G. Wang. "Heat transfer characteristics during jet impingement on a high-temperature plate surface" *Applied Thermal Engineering*, 100, (2016), 902-910
- S. G. Lee, M. Kaviany, C.-J. Kim and J. Lee. "Quasi-steady front in quench subcooled-jet impingement boiling: Experiment and analysis" *International Journal of Heat and Mass Transfer*, 113, (2017), 622-634
- A. K. Sharma, M. Modak and S. K. Sahu. "The heat transfer characteristics and rewetting behavior of hot horizontal downward facing surface by round water jet impingement" *Applied Thermal Engineering*, 138, (2018), 603-617
- C. Agrawal, R. Kumar, A. Gupta and B. Chatterjee. "Rewetting and maximum surface heat flux during quenching of hot surface by round water jet impingement" *International Journal of Heat and Mass Transfer*, 55, (2012), 4772-4782